A smartphone imaging-based label-free and dual-wavelength fluorescent biosensor with high sensitivity and accuracy

Won-Il Lee, Sajal Shrivastava, Le-Thai Duy, Bo Yeong Kim, Young-Min Son, Nae-Eung Lee

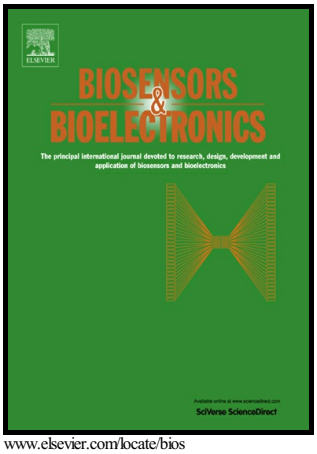

www.elsevier.com/locate/bios

PII: S0956-5663(17)30227-0
DOI: http://dx.doi.org/10.1016/j.bios.2017.03.061
Reference: BIOS9649

To appear in: *Biosensors and Bioelectronic*

Received date: 12 January 2017
Revised date: 16 March 2017
Accepted date: 29 March 2017

Cite this article as: Won-Il Lee, Sajal Shrivastava, Le-Thai Duy, Bo Yeong Kim, Young-Min Son and Nae-Eung Lee, A smartphone imaging-based label-free and dual-wavelength fluorescent biosensor with high sensitivity and accuracy *Biosensors and Bioelectronic,* http://dx.doi.org/10.1016/j.bios.2017.03.061

A smartphone imaging-based label-free and dual-wavelength fluorescent biosensor with high sensitivity and accuracy

Won-Il Lee[a], Sajal Shrivastava[b], Le-Thai Duy[b], Bo Yeong Kim[c], Young-Min Son[a], and Nae-Eung Lee[a,b,c*]

[a]Samsung Advanced Institute for Health Sciences & Technology (SAIHST), Sungkyunkwan University, 2066 Seobu-ro, Jangan-gu, Suwon, Gyeonggi-do 16419, Korea

[b]School of Advanced Materials Science & Engineering, Sungkyunkwan University, 2066 Seobu-ro, Jangan-gu, Suwon, Gyeonggi-do 16419, Korea

[c]SKKU Advanced Institute of Nanotechnology (SAINT), Sungkyunkwan University, 2066 Seobu-ro, Jangan-gu, Suwon, Gyeonggi-do 16419, Korea

[*]Corresponding author; E-mail: nelee@skku.edu

Abstract

The accuracy of a bioassay based on smartphone-integrated fluorescent biosensors has been limited due to the occurrence of false signals from non-specific reactions as well as a high background and low signal-to-noise ratios for complementary metal oxide semiconductor image sensors. To overcome this problem, we demonstrate dual-wavelength fluorescent detection of biomolecules with high accuracy. Fluorescent intensity can be quantified using dual wavelengths simultaneously, where one decreases and the other increases, as the target analytes bind to the split capture and detection aptamer probes. To do this, we performed smartphone imaging-based fluorescence microscopy using a microarray platform on a substrate with metal-enhanced fluorescence (MEF) using Ag film and Al_2O_3 nano-spacer. The results showed that the sensitivity and specificity of the dual-wavelength fluorescent quantitative assay for the target biomolecule 17-β-estradiol in water were significantly increased through the elimination of false

signals. The detection limit was 1 pg/mL and the area under the receiver operating characteristic curve of the proposed assay (0.922) was comparable to that of an enzyme-linked immunosorbent assay (0.956) from statistical accuracy tests using spiked wastewater samples. This novel method has great potential as an accurate point-of-care testing technology based on mobile platforms for clinical diagnostics and environmental monitoring.

Graphical abstract

We propose a new approach for high-accuracy quantitative detection of biomolecules based on a metal-enhanced dual-wavelength fluorescence imaging using a smartphone camera for practical applications. Bioassay tests with spiked samples of wastewater confirmed a high accuracy of the imaging-based fluorescent biosensor integrated with a smartphone, which is comparable to that of ELISA.

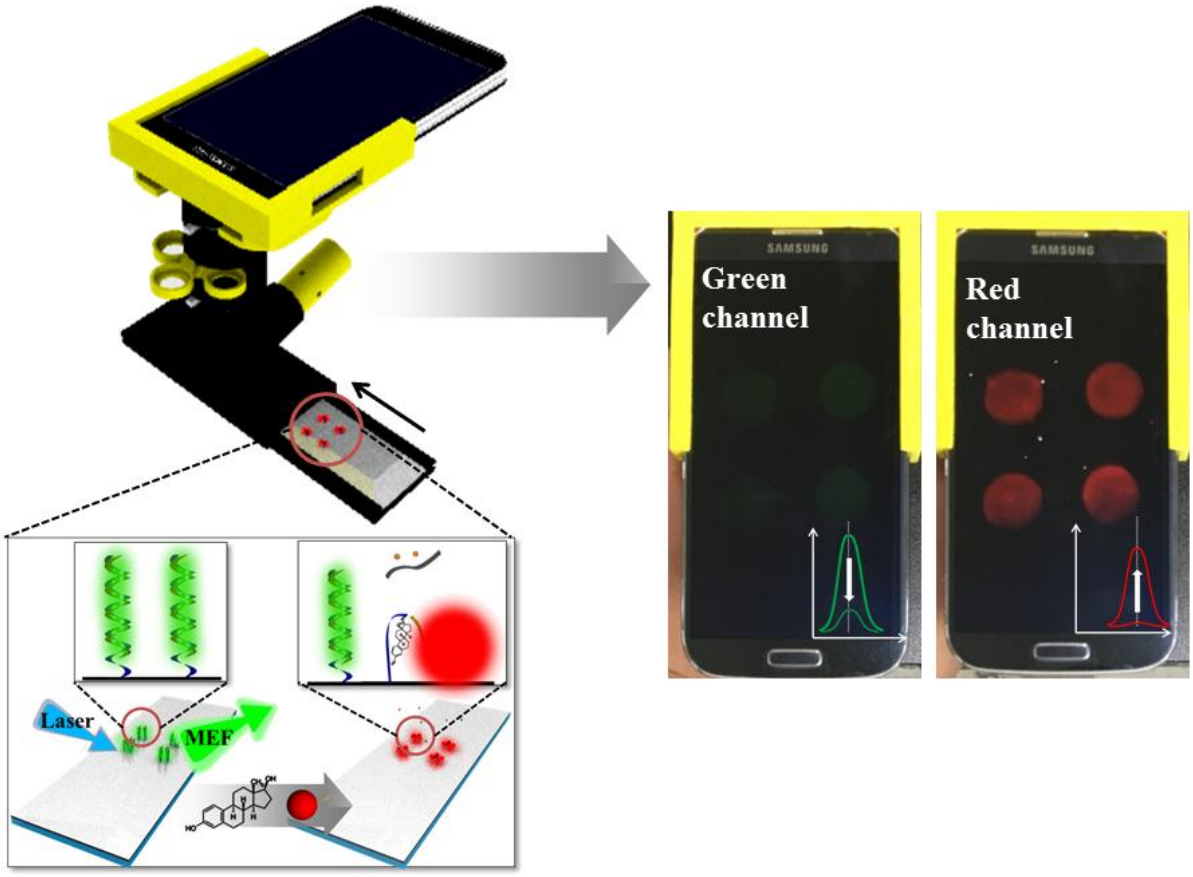

Keywords: Metal enhanced fluorescence, Fluorescent biosensor, Dual-wavelength, Split aptamer, Smartphone

1. Introduction

Since the smartphone was introduced, the specifications of the technology have strikingly progressed in all aspects, such as high-end complementary metal oxide semiconductor (CMOS)

digital cameras, powerful computing capability, wireless communication, compactness, and user-friendly interfaces. This fascinates researchers who work on portable and mobile biosensing systems for point-of-care testing (POCT) applications. In particular, a number of smartphone-integrated optical biosensing technologies have been developed due to the capability of optical biosensing devices to easily add-on to phone cameras. These technologies include bright-field imaging-based(Breslauer et al. 2009; D'Ambrosio et al. 2015; Guan et al. 2014), colorimetric(Choi et al. 2014; Chun et al. 2014; Laksanasopin et al. 2015; Mudanyali et al. 2012; Vashist et al. 2015), surface plasmonic resonance (SPR)(Liu et al. 2015; Preechaburana et al. 2012), and fluorescent biosensors(Barbosa et al. 2015; Koydemir et al. 2015; Ming et al. 2015; Noor and Krull 2014; Wei et al. 2013). Among various biosensing formats, colorimetric methods with simple optics have been studied more than others(McCracken and Yoon 2016), but have limitations in quantitative resolution that require complex systems for solving problems(Wang et al. 2017).

In many clinical and environmental assays, the fluorescent detection method has been preferred because it shows promise to achieve a low limit of detection (LOD), and it is simple to apply a multiplexed detection scheme(Petryayeva and Algar 2014) using different wavelengths of fluorophores. However, in most cases, smartphone-integrated fluorescent biosensors read out the fluorescent intensity change of only a single wavelength as the target concentration varies, leaving the assay vulnerable to inaccuracy due to false positive signals that can be caused by non-specific binding of the labeled probe to the sensor surface. Furthermore, an intrinsically (or extrinsically) elevated background signal can appear while capturing the true signal, even with stringent washing, because of a relatively low signal-to-noise ratio (SNR)(Balsam et al. 2015) for phone cameras with CMOS image sensors (CIS) used as bioassay readers compared to

conventional, highly sensitive, and large spectrophotometric instruments that have photomultiplier tubes (PMT) with high SNR as an optical detector. This can increase the occurrence of false negative signals. These factors make it harder for smartphone-integrated fluorescent biosensors to be commercialized since an inherently difficult challenge is complicated due to inaccuracy and imprecision(Vashist et al.).

In order to overcome such challenges, we propose a dual-wavelength fluorescent detection method(Shrivastava et al.) based on a split-aptamer microarray format with quantitative imaging-based fluorescent microscopy(Shrivastava et al. 2015) integrated with a smartphone. This method quantifies fluorescent signals from two wavelengths (one decreases, while the other increases as the target analytes bind to capture and detection split aptamers, respectively) to enhance the accuracy of biomolecular detection in microarray spots. This can reduce the chance of false detection significantly by excluding false positive (FP) and false negative (FN) signals within the sensing area, unlike the conventional method. This is because the true sensing reaction of target analytes accompanies the change of two wavelengths (green and red) in the fluorescence signal. Additionally, we utilized a substrate that employs silver-enhanced fluorescence(Sabanayagam and Lakowicz 2007; Wang et al. 2016) to compensate for the low SNR of CIS phone cameras for use as a fluorescence signal reader, which reduces FN signals by lowering the LOD. Combining the substrate modified by metal-enhanced fluorescence (MEF) technology and the dual-wavelength fluorescence detection scheme can reduce the occurrence of FN and FP signals, respectively, and, in turn, enhances the occurrence of true positive (TP) and true negative (TN) signals. As a result, the accuracy of the assay, which is commonly expressed as (TP + TN)/(TP + FP + FN + TN), can be increased. The related concept is depicted in **Table 1**.

Table 1. **Improvements in 4 test outcomes by the newly-designed mobile fluorescent assay**

		TP[a)]	FP [b)]	TN [c)]	FN [d)]
SNR of the fluorescence image by CIS	**Low (previous)**	↓ [f)]	.	.	↑[e)]
	High (current)	↑	.	.	↓
Wavelength for signal transduction	**Single (previous)**	↓	↑	↓	↑
	Dual (current)	↑	↓	↑	↓

[a)]TP: True positive,
[b)]FP: False positive,
[c)]TN: True negative,
[d)]FN: False negative,
[e)]↑ : high,
[f)]↓ : low

Estradiol, also known as 17-β-estradiol, was selected to demonstrate the dual-wavelength fluorescence quantitative biosensor. This molecule is the primary female estrogen sex hormone and regulates female menstrual reproductive cycles. Moreover, as a steroid, estradiol is also an endocrine disrupting chemical (EDC)(Chang et al. 2009), which interferes with the normal endocrine systems of organic life(Ying et al. 2002) and is found in public river water(Moraes et al. 2015; Trasande 2016). Therefore, it is beneficial to monitor estradiol levels for public health and ecological balance in wastewater in locations where simplified detection is needed for rapid response.

Herein, we demonstrate the dual-wavelength fluorescence quantitative detection of estradiol using an imaging-based fluorescent biosensor integrated with a smartphone. Specifically, we began with prototyping a custom-built fluorescent microscope using a 3D printer for smartphone integration as a mobile fluorescence reader and then built an accurate mobile biosensor on a fluorescence-enhanced microarray using two pieces of estradiol probe aptamer(Kim et al. 2007) made by splitting(Liu et al. 2014). Two different fluorescent signals

are reported from each piece of one target analyte, and the changes in each signal are compared. Furthermore, to validate the accuracy improvement that is achieved by using the dual-wavelength fluorescent detection on a portable add-on device, we conducted a biosensing test with spiked samples using wastewater and compared the accuracy of the test to the gold standard enzyme-linked immunosorbent assay (ELISA). The results showed a significant improvement in biosensing accuracy for the imaging-based fluorescent biosensor integrated with a smartphone, comparable to that of ELISA. This unique approach provides great potential for on-the-spot detection of biomolecules for environmental applications.

2. Experimental Procedures

2.1. Preparation of reagents

All reagents were purchased from Sigma Aldrich unless specifically noted. The DNA aptamer for estradiol was obtained split into cAP (5'-NH_2-$(CH_2)_6$-GCTTCCAGCTTATTGAATTACACGCAGAGGGTA-3') with its complementary sequence (5'-CGAAGGTCGAATAACTTAATGTGCGTCTCCCAT-3') and dAP (5'-NH_2-$(CH_2)_6$-CGAAGGCGCGAAGTCGCGCGTCGTTAACTTACGCGTCTCGGCG-3') from Integrated DNA Technologies. cAP was annealed with its complementary sequence by mixing with an equal molar concentration of 100 μM in 1× phosphate-buffered saline (PBS) buffer (pH 7.4), heating to 94 °C for 2 min, and cooling gradually. This stock solution was stored at -20 °C. About 10^{13} particles of Fluoresbrite® 50-nm YO carboxylate microspheres ($\lambda_{ex,\,max}$= 529/ $\lambda_{em,\,max}$ =546) purchased from Polyscience were activated with 2 mM 1-ethyl-3-(3-dimethyl aminopropyl)-carbodiimide (EDC) / 5 mM N-hydroxysuccinimide (NHS) in MES buffer (0.1 mM, pH 6) and cross-linked with 1mM dAP. 0.8% solution of agarose with low

electroendosmosis (EEO) for molecular biology in 1× Tris-Acetate-EDTA (TAE) buffer was casted into gel tray and agarose gel electrophoresis was run to purify the dAP-conjugated beads, and then the purified dAP-conjugated beads were suspended in Tris-buffered saline (TBS) buffer (100 mM Tri-HCl, 200 mM NaCl, 25 mM KCl, 10 mM $MgCl_2$, pH 8) and stored at 2~4 °C.

2.2. Fabrication of the microarray on the fluorescence-enhanced substrate

A 7.5 cm × 2.5 cm standard slide glass (Duran) was cleaned using the general RCA-1 cleaning process for 15 min. After drying with nitrogen, a 5-nm-thick Ti layer was deposited on the glass substrate as an adhesion layer and deposition of 120-nm-thick Ag thin film was followed by an e-beam evaporation system. Then, the Ag-coated substrate was loaded in the chamber of atomic layer deposition (ALD) system, and a 30-nm-thick Al_2O_3 film was deposited. Next, 3% (3-aminopropyl) triethoxysilane (APTES) in toluene aminated to the surface of the substrate for 30 min with controlled humidity (<50% RH) after hydroxylation through O_2 plasma using a chemical dry etcher for 30 s. Before the next step, the substrate was washed with toluene, ethanol, and distilled water in sequence 3 times each. Glutaraldehyde in PBS buffer (2.5 %, pH 7.4) formed aldehyde groups binding to amine groups, and the substrate was washed with distilled water. To prepare the micro-spotting ink, 16 μL of 10000× Sybr Green I (SGI) was added for intercalation in 2 mL of 10 μM double strand cAP in which 1.5 mM betaine and 0.005 % sarkosyl were dissolved. A cartridge containing 2 mL of ink was loaded in a Dimatix materials printer (DMP-2850, FUJIFILM), and 2 × 2 micro-spot array pattern (i.e., spot spacing and x, y dimensions) was designed by the provided computer software and printed in 16 layers on the center of the surface-modified substrate. cAP on the substrate was covalently bonded by incubating for 12 hrs, and then the substrate was washed stringently with 0.2 % sodium dodecyl

sulfate (SDS) dissolved in 1× PBS buffer, 1× PBS buffer, 0.05× PBS buffer, and distilled water sequentially.

2.3. Design and construction of the mobile fluorescence reader

The 3D design of the reader was based on the Samsung Galaxy S4 smartphone, drawn with Rhinoceros, essentially prefabricated and printed by a 3D printer (Replicator 2, Makerbot). Collimator lens-equipped laser diode modules, 60 mW/488 nm for green and 80 mW/515 nm for red and powered by 2 AA batteries, and bandpass filters, λ_{em} = 520/10 nm and λ_{em} = 605/15 nm, respectively, were purchased from Laser Pointer Holic Lasersystems and Edmund optics, respectively. A portable microscope with 200× magnification obtained from Amazon was disassembled, and only the eyepiece and the objective lens were incorporated with the 3D-printed prefab housing, where adjustment of the focus is available through a focusing knob attachment.

2.4. Target sensing and quantitative analysis

A 2 × 2 microarray sensing substrate was first imaged in the green channel and then the red channel of a mobile fluorescence reader. After acquisition of the initial images at each channel, an incubation chamber (Grace Bio-Labs) was applied on the substrate, and 150 μL of a mixture of estradiol and dAP-conjugated beads (100 mM Tri-HCl, 200 mM NaCl, 25 mM KCl, 10 mM $MgCl_2$, 5 % ethanol, pH 8) was injected into the chamber and incubated for 30 min at 36 ºC. Stringent washing with 0.01% SDS dissolved in 1× TBS, 1× TBS, and 0.01× TBS with agitation followed, and the substrate was dried completely after the chamber was removed. The reacted microarray was imaged at each channel, and all images were analyzed with ImageJ on a desktop computer. In both channels, the average intensity of 4 spots in the post-reaction image

over the initial image after background noise correction, which represents the relative fluorescent intensity, was calculated to be used as a parameter for estradiol quantification and to construct a standard curve.

2.5. Estradiol assay from spiked wastewater samples

The wastewater samples were obtained from the wastewater treatment plant of SKKU, whose effluent flows into the Irwol Reservoir located in Suwon City, Korea. The sample aliquots were prepared for 20 cases of estradiol spiking. Spiked water samples were filtered twice using a 0.2 μm hydrophilic PTFE syringe filter (Advantec) before the assay. The quantification of the assay was carried out separately with ELISA and mobile estradiol sensor. The same spiked samples were used in both cases. For assay tests of the dual-wavelength mobile estradiol sensor, quantification analysis was performed according to the pre-defined process written in **Table S3** and detections were repeated until the third accurate result satisfied the matching threshold that is less than 5% coefficient of variation (CV) between concentration read-outs from green and red channel from each assay of the spiked samples. In the case of mobile biosensing by the single-wavelength method, the average of all measurements at each concentration was used for post data processing. SPSS (IBM) was used to obtain the ROC curve and its derivative parameters (i.e., AUC and SD) with test results from ELISA and mobile estradiol sensor.

2.6. Protocol of Estradiol ELISA assay

A competitive ELISA kit for estradiol detection in the water samples (TOKIWA CHEMICAL INDUSTRIES) was used for this work. Calibration and sample test were conducted according to manufacturer's instructions. 100 μL of filtrated estradiol-spiked samples with various concentrations was mixed with 100 μL of reconstituted estradiol-enzyme conjugate

solution. Then, 100 μL of the mixture was added into antibody-coated well and incubated for 1 h at room temperature. After repeated washing with each 300 μL of wash solution, 100 μL of 3,3',5,5'-tetramethylbenzidine (TMB) color solution was reacted for 30 min and then 100 μL of citric acid stop solution was added. The absorbance at 450 nm wavelength was measured by an optical spectrophotometer (BioTek Synergy HT reader) and an absorbance reading was calculated for estradiol concentration from pre-set standard curve. The mean of triplicates at each concentration was calculated for the test results.

3. Results and Discussion

3.1. Design of dual-wavelength fluorescent detection with smartphone imaging

A schematic illustration of the overall work design for the dual-wavelength fluorescent detection proposed here is depicted in **Figure 1**. Here, since our research goal is to realize a highly accurate and reliable fluorescent biosensor integrated on a smartphone for use as a mobile reader, we built upon a fluorescent detection method based on dual-wavelengths by adopting our previous study(Shrivastava et al.) that has demonstrated high accuracy for quantitative bioassays. We utilized a split DNA probe aptamer for estradiol, where one sequence is the split capture aptamer (cAP) hybridized with a complementary DNA (cDNA) sequence that is intercalated by SGI. This is micro-spotted and covalently linked to a fluorescence-enhanced substrate for microarray fabrication (**Figure 1a**). Meanwhile, a split detection aptamer (dAP) of another sequence is immobilized on label-free red fluorescent nanobeads that are intended for signal amplification and arranged in a ready-to-use reagent (**Figure S1**). According to the estradiol concentration, SGI is released by dehybridization of cAP, while cAP, estradiol, and the dAP-conjugated beads form a complex due to specific affinity. This causes a decrease in green

fluorescence from cAP and an increase in red fluorescence from dAP on the microarray (**Figure 1b**). After the microarray substrate is inserted into the mobile fluorescence reader (**Figure 1c**), the reaction was simultaneously analyzed and quantified by capturing fluorescent images (**Figure 1d**) using a CIS phone camera to assess the LOD and the dynamic range of the sensor (**Figure 1e**).

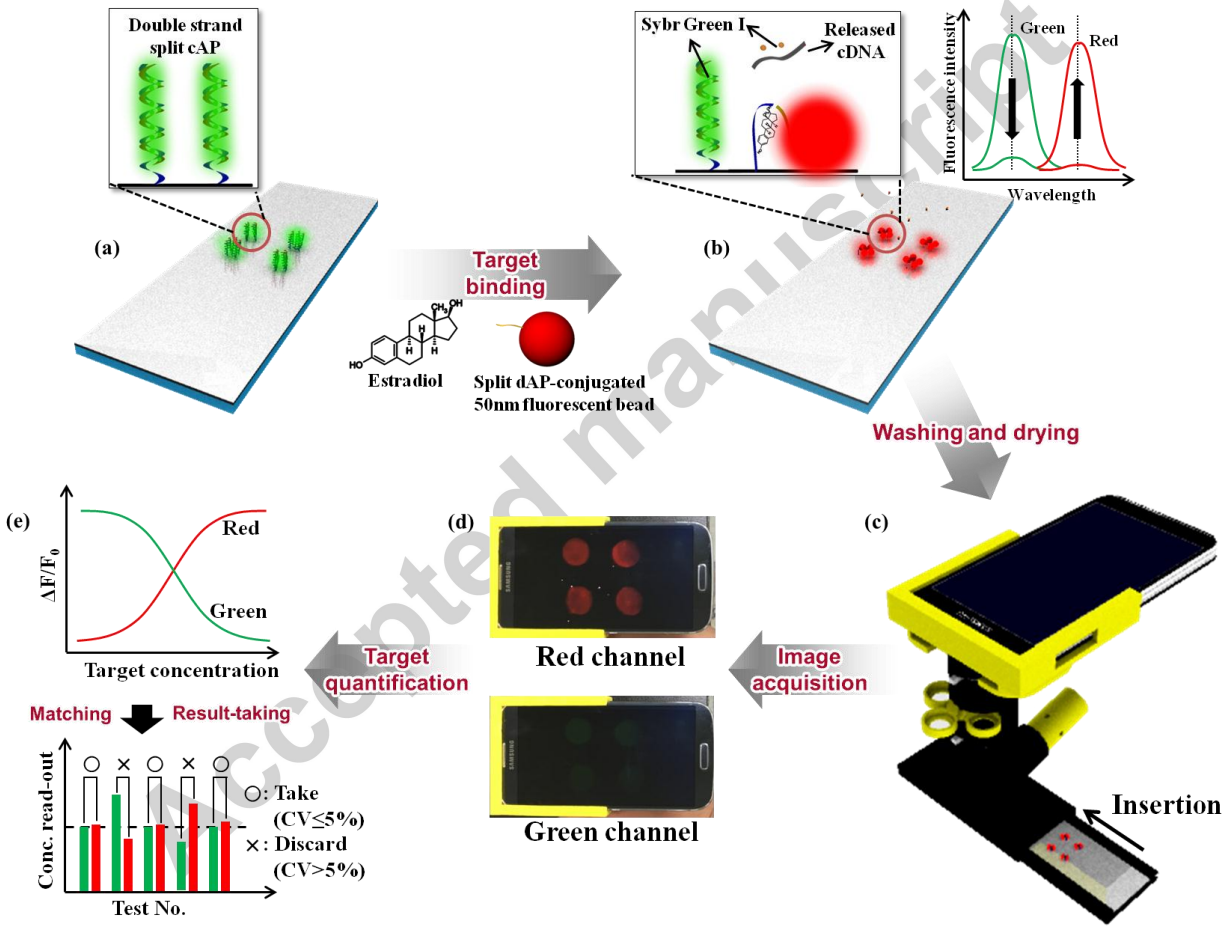

Fig. 1. Schematic illustration of the overall work design. *(a) Micro-spots of cAP hybridized with cDNA and intercalated by SGI are printed and cross-linked on a microarray on the fluorescence-enhanced substrate. (b) Once estradiol and dAP-conjugated fluorescent beads interact on the microarray, green fluorescence from cAP decreases, releasing cDNA and SGI,*

but red fluorescence from dAP increases with target binding. (c) The glass substrate with the microarray is inserted into the mobile reader. (d) Fluorescent images at the red and green channels are acquired. (e) The change in fluorescent intensity at each channel is analyzed and a matching process for selection of the reliable outcome was carried out. A test result with the matched ratio within a particular CV value was taken for the reliable result and quantification.

3.2. Use of a fluorescence-enhanced substrate

Unlike scientific digital cameras with scientific CMOS (sCMOS) and charge-coupled device (CCD) image sensors, the camera embedded in a smartphone has a considerable noise level(Zhou et al. 2014) in low-light images like fluorescent images. This may lead to a decrease in accuracy for quantitative fluorescent biosensing due to its low SNR, causing an increase of false negative signals during the assay. As a breakthrough, a fluorescent signal-enhanced substrate was utilized to complement the low fluorescence detection sensitivity of a phone camera and increase the signal in the image. In this work, metal-enhanced fluorescence (MEF) achieved by a thin Ag layer on a glass substrate was introduced as a main method to enhance the fluorescent signal. **Figure 2a** shows the fabrication procedure for the fluorescence-enhanced substrate, which consisted of a Ag thin film (~120 nm) and an ultrathin Al_2O_3 nano-spacer (~30 nm) deposited as a nano-spacer on a standard slide glass (the optimization of the thickness of the Al_2O_3 nano-spacer is shown in **Supporting Figures S2b**). The optimum enhancement for fluorescent emission occurs by coupling optical resonance with surface plasmons and inducing high radiative decay of fluorophores with Purcell effect from Ag layer (field-emission scanning electron microscopy (FE-SEM) image is shown in **Supporting Figure S2a**) that has 30-nm-thick Al_2O_3 nano-spacer on the surface.(Aslan et al. 2005; Cheng and Xu 2007; Sabanayagam and

Lakowicz 2007) To confirm the signal enhancement by MEF, 1 μL of SGI-intercalated double-strand DNA with an amine group at one end of the sequence was covalently immobilized on the substrate after a series of surface modifications. Fluorescent enhancement of the substrate is visually observed in the fluorescent image with clarity compared to the fluorescence intensity from bare slide glass (**Figure 2b**). This image was taken by a cooled CCD camera (XM-10) integrated on a bench-top fluorescent microscope (Olympus IX-81). As shown in **Figure 2c**, the enhancement factor of fluorescent emission on the Ag-coated MEF substrate is approximately 14.5 times higher than that on bare slide glass, as determined by densitometric measurements with the same region of interest (ROI). Importantly, this fluorescent-enhanced substrate allows us to take fluorescent images with increased intensity so that we can realize a quantitative biosensor using dual-wavelength fluorescent detection comprised of a low LOD and broad dynamic range through a phone camera since a bare slide glass substrate cannot generate enough intensity for detection.

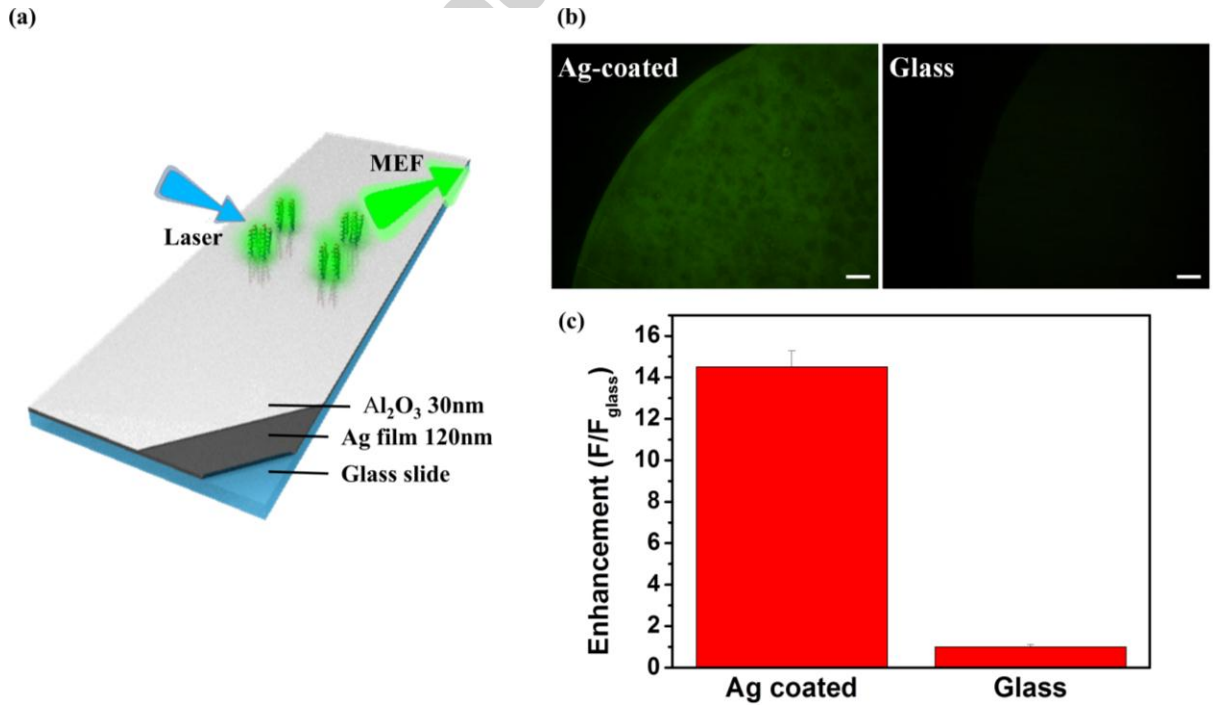

Fig. 2. Schematics for fabrication of the fluorescence-enhanced substrate and confirmation of enhancement. *(a) 120-nm-thick Ag and 30-nm-thick Al_2O_3 thin films, which are mainly for MEF, are deposited on slide glass in sequence to make a fluorescence-enhanced substrate, and a series of cross-linking chemical reactions are applied for SGI-intercalated hybridized DNA immobilization. Fluorescence enhancement of the substrate was confirmed by comparing it to bare slide glass qualitatively with the fluorescent images in (b) and quantitatively with the densitometric measurements in (c), showing that the level of enhancement is approximately 14.5 times.*

3.3. Smartphone imaging-based mobile fluorescence reader

We prototyped a customized portable fluorescence microscope using the digital camera of a Samsung Galaxy S4 smartphone, which is capable of taking crisp fluorescent images with high magnification. **Figure 3a** depicts the essential parts that composed the microscope. The microscope body was designed in the shape of a cylindrical pipe to contain an objective lens and an eyepiece at the middle and top, respectively. A focusing knob is attached to the objective lens directly, and housing on the bottom allows for insertion of the fluorescence-enhanced substrate mounted on the sensor case. Between the eyepiece and the objective lens, bandpass filters that filter emission wavelengths are mounted on a quadruple filter case and then assembled, revolved and aligned to the imaging axis according to the green or red channel modes. A low incident angle of the laser (13°) was critical to suppress background noise because the Ag-coated glass substrate is highly reflective, which can misguide the reflected or scattered excitation light source toward the lens in an upright microscope. To capture the fluorescence image, a 60

mW/488 nm laser diode module in a laser sheath and an emission filter (λ_{em} = 520/10 nm) were used for the green channel; likewise, an 80 mW/515 nm laser diode and an emission filter (λ_{em} = 605/15 nm) were used for the red channel. After inserting the mounted fluorescence-enhanced substrate on which SGI-intercalated double-strand DNA aptamers are micro-arrayed using an inkjet printer, a 2 × 2 micro-spot array was placed in the center of the field of view (FOV) and imaged on the green channel (**Figure 3b**). The advantages of utilizing the 2 × 2 microarray format for fluorescent biosensing are that, first, we can calculate the intensity change by a target analyte in the fixed sensing area within the FOV, and second, the intensity averaged for 4 micro-spots is able to compensate for signal outliers. Hence, when imaging, the uniform distribution of fluorescent intensity within the FOV on the as-prepared sensing substrate must be addressed to obtain a reliably high accuracy of detection. As shown in **Figure 3c**, 4 micro-spots in the 2 × 2 microarray image taken by the mobile fluorescence reader have visually and quantitatively uniform intensity profiles along the 400 × 400 pixels that are contained in each spot (**Figure 3d**).

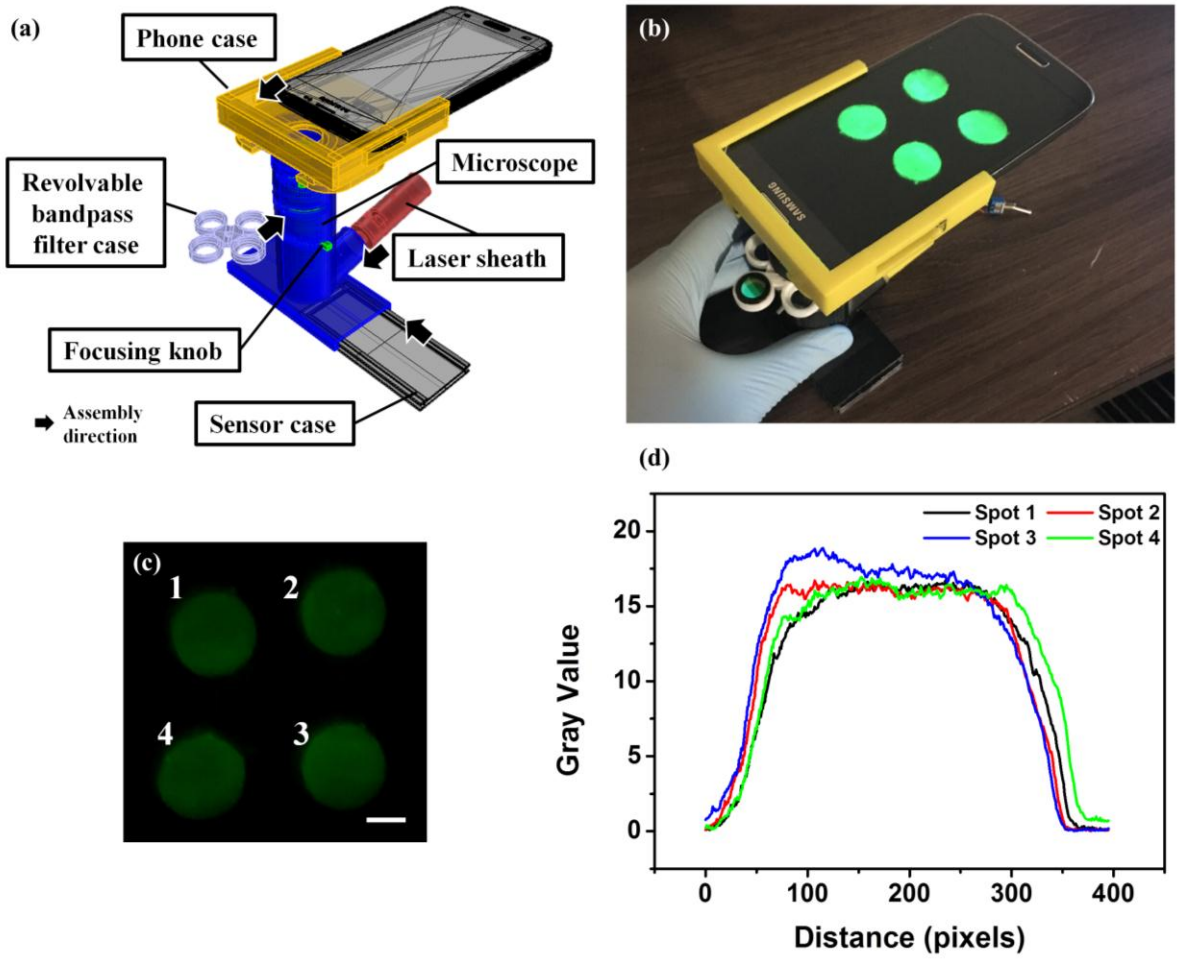

Fig. 3. Prototyping of the mobile fluorescence reader and its quality of fluorescent imaging. *(a) Black and white rendering of the mobile fluorescence reader with labeling for each functioning part. A demonstration of fluorescent imaging with a real object is shown in (b). (c) Fluorescent image of micro-spots in the green channel taken by the mobile reader (scale bar, 50 μm). (d) Plot profiling of each micro-spot containing 400×400 pixels. The spot numbers correspond to the numbers in (c).*

3.4. Quantification of estradiol using the mobile fluorescence reader

Our biosensing design, in combination with the planar fluorescence-enhanced sensing substrate and imaging-based mobile reader, is favorable for highly sensitive and precise detection. This is because it provides a setting that is much closer to absolute quantification by projecting a two-dimensional sensing plane directly onto the image sensor without an out-of-focus background. Adapting a split aptamer for the target analyte estradiol, which has proven selectivity and sensitivity(Fan et al. 2014; Kim et al. 2007; Liu et al. 2014), we demonstrated biosensing with a serial dilution of estradiol and constructed a standard curve. Initially, imaging on the green channel where SGI is fully loaded in the double-strand cAP on a blank sample showed the highest fluorescent intensity representing the normally-on type biosensor. This revealed that the intensity decreases as the concentration of estradiol increases. In contrast, it was observed that the fluorescent signal intensity on the red channel increases with self-assembly of the dAP-conjugated red fluorescent beads, cAP, and estradiol according to escalating target concentration, which did not experience fluorescence bleed-through between the two channels (**Figure 4a**). To calibrate batch-to-batch calculations of signal intensity related to target concentration, we used relative fluorescent intensity ($\Delta F/F_0$), which is the intensity change post-reaction over the initial intensity, instead of absolute values. The standard curves for estradiol were constructed from two green and red channels (**Figures 4b and 4c**), which have a corresponding dynamic range from 1 pg/mL to 100 ng/mL. The linear response of the biosensing spans the dynamic range where the green and red channels resulted in the LOD of 1 pg/mL with a signal level of 0.93 ± 0.023 / 1.28 ± 0.122 and saturated at 100 ng/mL (0.12 ± 0.048 / 12.79 ± 1.13), respectively. Importantly, the value of the LOD is low enough to conduct a bioassay test in the field since the level of estradiol that can disturb the ecosystem(Kang et al. 2002) and be

monitored in the water supply in a certain country(Wakayama 2003) extends to a few tens of pg/mL.

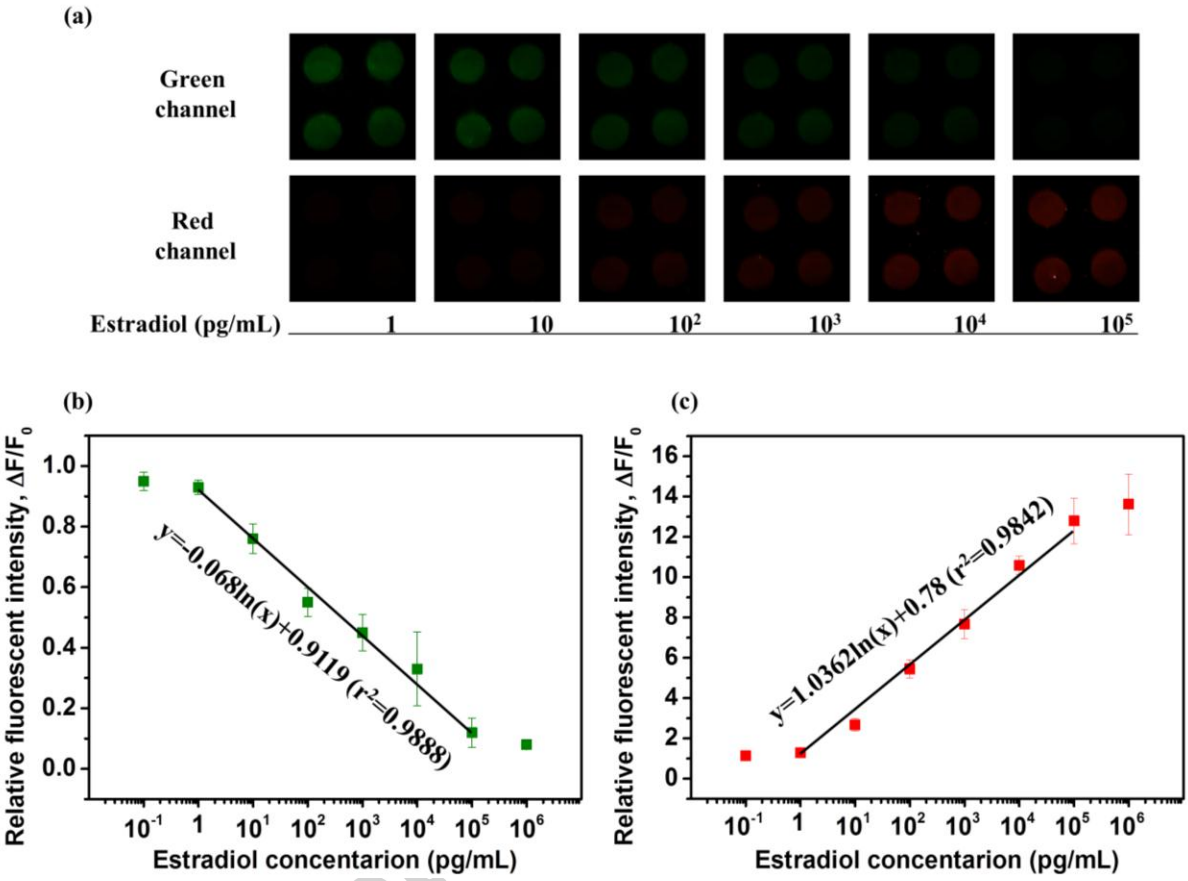

Fig. 4. Analytical characteristics of relative fluorescence intensity versus estradiol concentration on the green and red channels measured by the mobile biosensor. *(a) It is clearly observed that the fluorescent intensity decreases in green channel and increases in red channel with escalating estradiol addition. The linear range is plotted for (b) the green channel and (C) the red channel. At all points, measurements were triplicated. These two calibration curves are used for simultaneous quantification of estradiol.*

3.5. Accuracy verification of bioassays for estradiol detection with real samples

We performed a statistical bioassay test to investigate how the detection method applied to our mobile fluorescent biosensor can increase the accuracy by using real spiked samples and comparing the results to that of an ELISA test, which has not been conducted before. Estradiol molecules were spiked into wastewater collected from a wastewater treatment plant. Since an estradiol concentration over 80 pg/mL is considered to be problematic in a water supply(Wakayama 2003), we selected spiking concentrations that centered around this level and set it as the cut-off value at which detection results are determined to be positive or negative. **Tables S1 and S2** show the comparison in recovery rate of the same 20 spiked samples (n=3) quantified with ELISA and our dual-wavelength mobile biosensor, respectively. We observed that the recovery rate achieved by the mobile biosensor showed little difference, only 4.19% lower at the minimum and 6.05% higher at the maximum, from the outcome of ELISA test and retained a CV below 10% for each sample. In the scattered plot of 19 samples (excluding 0 pg/mL), the sensitivity (the ratio of true-positives, TP/(TP + FP)) and specificity (the ratio of true-negatives, TN/(TN + FN)) of the assay were 77.8% and 80%, respectively, with two more false negatives and one more false positive than the ELISA test (**Figures 5a and 5b**). Note that such values of sensitivity and specificity in detection of small biomolecules with a smartphone-based optical biosensor have not been recorded to date. Comparison of the accuracy between the two assay tests is clearly shown in **Figure 5c** in terms of the area under the receiver operating characteristic (ROC) curve (AUC), which is a general indication of accuracy in a diagnostic test(Zhou et al. 2011). The AUC of our mobile biosensor (0.922) was close to that of ELISA (0.956), which indicates that the detection distinguishes among the samples even at intervals of 1 pg/mL with positive and negative signals based on the cut-off value. As mentioned previously, the dual-wavelength fluorescent detection method is advantageous to obtain better accuracy in

detection by matching two fluorescent signals within a certain CV limit for a target analyte or discarding otherwise. The key to understanding how the accuracy of the test is enhanced is using a CV limit to match signals from the green and red channels. This is because matching two signals for quantification of a target analyte plays a role in selecting measurement results close to an actual concentration with a low CV limit. For example, the mean value of each concentration read-out from the two channels only below a certain percentage of CV is taken as a final result, while all concentration read-outs above the CV that are probably caused by ununiform fabrication of the substrate, pipetting or device handling etc. are discarded. In our case, by quantifying results with a 5% CV limit only, which is a ratio of the difference in read-outs from the two channels, and using their mean value for every spiked sample, we could filter out inaccurate outcomes (40 of 100 total measurements) as shown in **Supporting Figure S4**. It is confirmed that dual-wavelength detection outperformed single-wavelength detection regarding the accuracy of our mobile biosensor for estradiol detection, as shown in the comparative data in **Table 2** and **Supporting Figure S3**. The AUC values in the single-wavelength detection method are 0.833 from the green channel and 0.822 from the red channel and are accompanied by lower sensitivity, lower specificity. and higher standard deviation (SD) compared to the high accuracy of the dual-wavelength detection method.

Table 2. Accuracy comparison of the statistical bioassay test according to detection method

Detection method		Sensitivity(%)	Specificity(%)	AUC	SD
ELISA		88.9	100	0.956	0.048
Dual-wavelength		77.8	80	0.922	0.064
Single-wavelength	Green channel	66.7	70	0.833	0.98
	Red channel	66.7	60	0.822	0.99

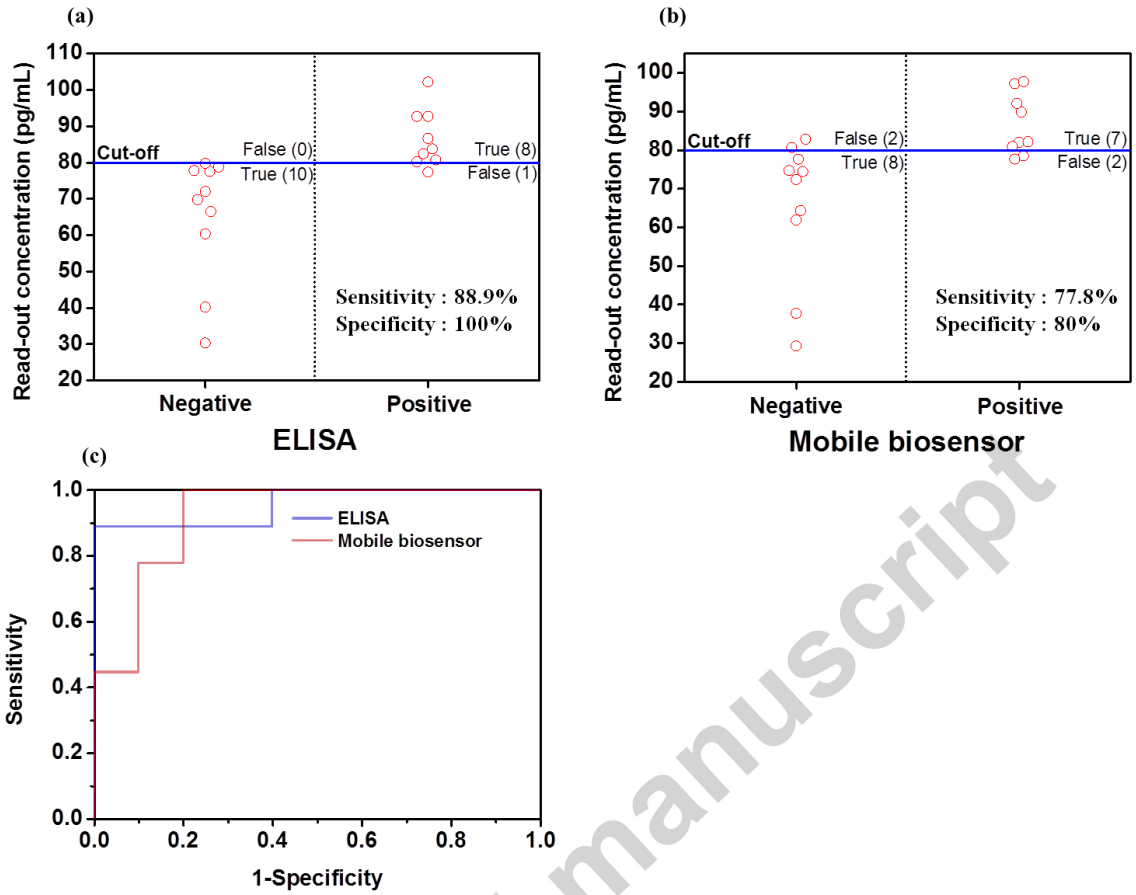

Fig. 5. Statistical bioassay test of estradiol detection for the mobile biosensor compared to ELISA. *The scatter plot displays how detection results are distributed in negative and positive groups for (a) ELISA and (b) the mobile biosensor. Each point is the mean of the triplicate measurements. (c) Comparison of ROC curves between ELISA and the mobile biosensor.*

4. Conclusions

Here, we introduced a smartphone imaging-based fluorescent biosensor that is capable of detecting small biomolecules such as estradiol with high accuracy, i.e., high sensitivity and selectivity. For high sensitivity of the mobile bioassay for estradiol in wastewater, we utilized a fluorescence-enhanced substrate, applying MEF to enhance the signal to a level that is

approximately 14.5 times higher than that of bare slide glass, and for which the LOD could reach as low as 1 pg/mL. This was integrated onto a prototyped mobile fluorescence reader with an excitation light source at a low incident angle relative to the sensing substrate. For high selectivity of the bioassay, the dual-wavelength detection method was used on an aptamer microarray, with fluorescent imaging on two channels (green and red) of a mobile reader. Utilizing this new approach, an estradiol assay based on the dual-wavelength mobile fluorescent biosensor resulted in high accuracy (AUC=0.922) comparable to that of ELISA (AUC=0.956). By achieving this high accuracy, our approach can provide a breakthrough for unmet demands related to accuracy and precision for commercialization of a mobile fluorescent biosensor that is integrated with a smartphone.

Acknowledgments

This research was supported by the Nano Material Technology Development Program (NRF-2016M3A7B4910554) and Global Ph.D Fellowship Program (NRF-2015H1A2A1034159) through the National Research Foundation of Korea (NRF).

References:

Aslan, K., Leonenko, Z., Lakowicz, J.R., Geddes, C.D., 2005. Annealed Silver-Island Films for Applications in Metal-Enhanced Fluorescence: Interpretation in Terms of Radiating Plasmons. Journal of Fluorescence 15(5), 643.

Balsam, J., Bruck, H.A., Rasooly, A., 2015. Smartphone-Based Fluorescence Detector for mHealth. In: Rasooly, A., Herold, K.E. (Eds.), Mobile Health Technologies: Methods and Protocols, pp. 231-245. Springer New York, New York, NY.

Barbosa, A.I., Gehlot, P., Sidapra, K., Edwards, A.D., Reis, N.M., 2015. Portable smartphone quantitation of prostate specific antigen (PSA) in a fluoropolymer microfluidic device. Biosensors and Bioelectronics 70, 5-14.

Breslauer, D.N., Maamari, R.N., Switz, N.A., Lam, W.A., Fletcher, D.A., 2009. Mobile Phone Based Clinical Microscopy for Global Health Applications. PLoS ONE 4(7), e6320.

Chang, H.-S., Choo, K.-H., Lee, B., Choi, S.-J., 2009. The methods of identification, analysis, and removal of endocrine disrupting compounds (EDCs) in water. Journal of Hazardous Materials 172(1), 1-12.

Cheng, D., Xu, Q.-H., 2007. Separation distance dependent fluorescence enhancement of fluorescein isothiocyanate by silver nanoparticles. Chemical Communications(3), 248-250.

Choi, S., Kim, S., Yang, J.-S., Lee, J.-H., Joo, C., Jung, H.-I., 2014. Real-time measurement of human salivary cortisol for the assessment of psychological stress using a smartphone. Sensing and Bio-Sensing Research, 8-11.

Chun, H.J., Park, Y.M., Han, Y.D., Jang, Y.H., Yoon, H.C., 2014. Paper-based glucose biosensing system utilizing a smartphone as a signal reader. BioChip Journal 8(3), 218-226.

D'Ambrosio, M.V., Bakalar, M., Bennuru, S., Reber, C., Skandarajah, A., Nilsson, L., Switz, N., Kamgno, J., Pion, S., Boussinesq, M., Nutman, T.B., Fletcher, D.A., 2015. Point-of-care quantification of blood-borne filarial parasites with a mobile phone microscope. Science Translational Medicine 7(286), 286re284-286re284.

Fan, L., Zhao, G., Shi, H., Liu, M., Wang, Y., Ke, H., 2014. A Femtomolar Level and Highly Selective 17β-estradiol Photoelectrochemical Aptasensor Applied in Environmental Water Samples Analysis. Environmental Science & Technology 48(10), 5754-5761.

Guan, L., Tian, J., Cao, R., Li, M., Cai, Z., Shen, W., 2014. Barcode-Like Paper Sensor for Smartphone Diagnostics: An Application of Blood Typing. Analytical Chemistry 86(22), 11362-11367.

Kang, I.J., Yokota, H., Oshima, Y., Tsuruda, Y., Yamaguchi, T., Maeda, M., Imada, N., Tadokoro, H., Honjo, T., 2002. Effect of 17β-estradiol on the reproduction of Japanese medaka (Oryzias latipes). Chemosphere 47(1), 71-80.

Kim, Y.S., Jung, H.S., Matsuura, T., Lee, H.Y., Kawai, T., Gu, M.B., 2007. Electrochemical detection of 17β-estradiol using DNA aptamer immobilized gold electrode chip. Biosensors and Bioelectronics 22(11), 2525-2531.

Koydemir, H.C., Gorocs, Z., Tseng, D., Cortazar, B., Feng, S., Chan, R.Y.L., Burbano, J., McLeod, E., Ozcan, A., 2015. Rapid imaging, detection and quantification of Giardia lamblia cysts using mobile-phone based fluorescent microscopy and machine learning. Lab on a Chip 15(5), 1284-1293.

Laksanasopin, T., Guo, T.W., Nayak, S., Sridhara, A.A., Xie, S., Olowookere, O.O., Cadinu, P., Meng, F., Chee, N.H., Kim, J., Chin, C.D., Munyazesa, E., Mugwaneza, P., Rai, A.J., Mugisha,

V., Castro, A.R., Steinmiller, D., Linder, V., Justman, J.E., Nsanzimana, S., Sia, S.K., 2015. A smartphone dongle for diagnosis of infectious diseases at the point of care. Science Translational Medicine 7(273), 273re271-273re271.

Liu, J., Bai, W., Niu, S., Zhu, C., Yang, S., Chen, A., 2014. Highly sensitive colorimetric detection of 17β-estradiol using split DNA aptamers immobilized on unmodified gold nanoparticles. Scientific Reports 4, 7571.

Liu, Y., Liu, Q., Chen, S., Cheng, F., Wang, H., Peng, W., 2015. Surface Plasmon Resonance Biosensor Based on Smart Phone Platforms. Scientific Reports 5, 12864.

McCracken, K.E., Yoon, J.-Y., 2016. Recent approaches for optical smartphone sensing in resource-limited settings: a brief review. Analytical Methods 8(36), 6591-6601.

Ming, K., Kim, J., Biondi, M.J., Syed, A., Chen, K., Lam, A., Ostrowski, M., Rebbapragada, A., Feld, J.J., Chan, W.C.W., 2015. Integrated Quantum Dot Barcode Smartphone Optical Device for Wireless Multiplexed Diagnosis of Infected Patients. ACS Nano 9(3), 3060-3074.

Moraes, F.C., Rossi, B., Donatoni, M.C., de Oliveira, K.T., Pereira, E.C., 2015. Sensitive determination of 17β-estradiol in river water using a graphene based electrochemical sensor. Analytica Chimica Acta 881, 37-43.

Mudanyali, O., Dimitrov, S., Sikora, U., Padmanabhan, S., Navruz, I., Ozcan, A., 2012. Integrated rapid-diagnostic-test reader platform on a cellphone. Lab on a Chip 12(15), 2678-2686.
Noor, M.O., Krull, U.J., 2014. Camera-Based Ratiometric Fluorescence Transduction of Nucleic Acid Hybridization with Reagentless Signal Amplification on a Paper-Based Platform Using Immobilized Quantum Dots as Donors. Analytical Chemistry 86(20), 10331-10339.

Petryayeva, E., Algar, W.R., 2014. Multiplexed Homogeneous Assays of Proteolytic Activity Using a Smartphone and Quantum Dots. Analytical Chemistry 86(6), 3195-3202.

Preechaburana, P., Gonzalez, M.C., Suska, A., Filippini, D., 2012. Surface Plasmon Resonance Chemical Sensing on Cell Phones. Angewandte Chemie 124(46), 11753-11756.

Sabanayagam, C.R., Lakowicz, J.R., 2007. Increasing the sensitivity of DNA microarrays by metal-enhanced fluorescence using surface-bound silver nanoparticles. Nucleic Acids Research 35(2), e13-e13.

Shrivastava, S., Sohn, I.-Y., Son, Y.-M., Lee, W.-I., Lee, N.-E., 2015. Real-time label-free quantitative fluorescence microscopy-based detection of ATP using a tunable fluorescent nano-aptasensor platform. Nanoscale 7(46), 19663-19672.

Shrivastava, S., Triet, N.M., Son, Y.-M., Lee, W.-I., Lee, N.-E., Seesawed fluorescence nano-aptasensor based on highly vertical ZnO nanorods and three-dimensional quantitative fluorescence imaging for enhanced detection accuracy of ATP. Biosensors and Bioelectronics.

Trasande, L., 2016. Stand firm on hormone disruptors. Nature 539(7630), 469.

Vashist, S.K., Luppa, P.B., Yeo, L.Y., Ozcan, A., Luong, J.H.T., Emerging Technologies for Next-Generation Point-of-Care Testing. Trends in Biotechnology 33(11), 692-705.

Vashist, S.K., van Oordt, T., Schneider, E.M., Zengerle, R., von Stetten, F., Luong, J.H.T., 2015. A smartphone-based colorimetric reader for bioanalytical applications using the screen-based bottom illumination provided by gadgets. Biosensors and Bioelectronics 67, 248-255.

Wakayama, H., 2003. Revision of Drinking Water Quality Standards in Japan. Japan MHLW, Japan MHLW.

Wang, L.-J., Chang, Y.-C., Sun, R., Li, L., 2017. A multichannel smartphone optical biosensor for high-throughput point-of-care diagnostics. Biosensors and Bioelectronics 87, 686-692.

Wang, Y., Li, H., Xu, D., 2016. Aptamers-based sandwich assay for silver-enhanced fluorescence multiplex detection. Analytica Chimica Acta 905, 149-155.

Wei, Q., Qi, H., Luo, W., Tseng, D., Ki, S.J., Wan, Z., Göröcs, Z., Bentolila, L.A., Wu, T.-T., Sun, R., Ozcan, A., 2013. Fluorescent Imaging of Single Nanoparticles and Viruses on a Smart Phone. ACS Nano 7(10), 9147-9155.

Ying, G.-G., Kookana, R.S., Ru, Y.-J., 2002. Occurrence and fate of hormone steroids in the environment. Environment International 28(6), 545-551.

Zhou, X.-H., Obuchowski, N.A., McClish, D.K., 2011. Statistical Methods in Diagnostic Medicine, 2nd Edition ed. WILEY, New York.

Zhou, X., Wong, T.I., Song, H.Y., Wu, L., Wang, Y., Bai, P., Kim, D.-H., Ng, S.H., Tse, M.S., Knoll, W., 2014. Development of Localized Surface Plasmon Resonance-Based Point-of-Care System. Plasmonics 9(4), 835-844.

Highlights

- Method for enhanced detection accuracy of mobile fluorescent aptasensor was proposed.
- Substrate with metal-enhanced fluorescence (MEF) reduced false negative signals with lowered detection limit by compensating low signal-to-noise ratio of CMOS camera
- Dual-wavelength fluorescent detection on microarray format was applied as a biosensig scheme to eliminate false positive and negative signals.
- Statistical detection test with spiked 17-β-estradiol samples confirmed enhanced detection accuracy of the mobile biosensor compared to ELISA